Mon. Not. R. Astron. Soc. **338,** 623–636 (2003)

# Predictions for statistical properties of forming spheroidal galaxies

F. Perrotta,[1,2⋆] M. Magliocchetti,[2] C. Baccigalupi,[2] M. Bartelmann,[3] G. De Zotti,[1] G. L. Granato,[1] L. Silva[4] and L. Danese[2]

[1]*Osservatorio Astronomico di Padova, Vicolo dell'Osservatorio 5, I-35122 Padova, Italy*
[2]*SISSA/ISAS, Via Beirut 4, I-34014 Trieste, Italy*
[3]*Max-Planck Institut für Astrophysik, PO Box 1317, D-85741 Garching, Germany*
[4]*Osservatorio Astronomico di Trieste, Via G. B. Tiepolo 11, I-34131 Trieste, Italy*

Accepted 2002 September 15. Received 2002 August 26; in original form 2002 November 16



**ABSTRACT**

We show that the features of the recent astrophysically motivated model by Granato et al. are fully consistent with the available statistical measurements of galaxies at (sub)millimetre wavelengths. We quantitatively predict the impact of this scenario on near-future cosmological observations dealing with spatial and flux statistical distribution of (sub)millimetre galaxies. We show that the expected angular correlation function of spheroids is compatible with available data. We compute the expected power spectrum of fluctuations due to clustering at the frequencies of the High Frequency Instrument (HFI) on ESA's *Planck* satellite: the clustering signal is found to be detectable in regions of low interstellar dust emission.

A further distinctive prediction of the adopted model is a remarkably high fraction of gravitationally lensed sources at bright millimetre/submillimetre fluxes. In fact, since most spheroids burn at redshift $z \simeq 2$–3 according to the adopted model, gravitational lensing amplifies a significant number of high-$z$ forming spheroidal galaxies, which will be detectable by large-area, shallow surveys at millimetre/submillimetre wavelengths, such as those carried out by *Planck*/HFI. Allowing for other source populations, we find that the fraction of gravitationally lensed millimetre/submillimetre sources at fluxes $>100$ mJy is expected to be up to $\simeq$40 per cent.

**Key words:** gravitational lensing – galaxies: formation – large-scale structure of Universe – submillimetre.

## 1 INTRODUCTION

The formation and early evolution of massive spheroidal galaxies is still a most controversial issue (see e.g. Peebles 2002, for a recent review). In the general framework of the hierarchical clustering picture for structure formation in cold dark matter (CDM) cosmologies, two scenarios are confronting each other. According to the 'monolithic' scenario, a large fraction of giant elliptical galaxies formed most of their stars in a single gigantic starburst at high redshift, and then essentially underwent passive evolution. This approach is in contrast with the 'merging' scenario, backed up by semi-analytic galaxy formation models (e.g. Kauffmann 1996; Baugh et al. 1998), wherein large galaxies mostly formed via mergers of smaller sub-units that, at the time of merging, had already converted part of their gas into stars. These two scenarios yield very different predictions for the evolution of large ellipticals: If 'monolithic' collapse is assumed, the comoving number density of such galaxies remains essentially constant with redshift, while their bolometric luminosity increases with look-back time out to their epoch of formation. On the contrary, according to the 'merging' scenario, the comoving density of large ellipticals decreases with increasing redshift.

The evolution of the comoving density in the optical band has, however, proven difficult to measure, and discordant results have been reported. A deficit of old ellipticals at $z \gtrsim 1$, when compared to predictions from pure luminosity evolution models, has been claimed by several groups (Kauffmann, Charlot & White 1996; Zepf 1997; Franceschini et al. 1998; Barger et al. 1999b; Menanteau et al. 1999; Treu & Stiavelli 1999; Rodighiero, Franceschini & Fasano 2001), while others found evidence for a constant comoving density up to $z \sim 1.5$ (Totani & Yoshii 1997; Benitez et al. 1999; Broadhurst & Bowens 2000; Scodeggio & Silva 2000; Cohen 2001). Furthermore, Daddi, Cimatti & Renzini (2000) find that the observed surface density of extremely red objects (EROs) – the bulk of which appear to be passively evolving ellipticals – is consistent with predictions from the 'monolithic' scenario.

The results of SCUBA and MAMBO surveys at submillimetre/millimetre (sub-mm/mm) wavelengths present a challenge for

⋆E-mail: perrotta@sissa.it

the current versions of semi-analytical models. The most exhaustive investigation carried out so far (Granato et al. 2000) combines the semi-analytic galaxy formation model by the Durham group (Cole et al. 2000) with the state-of-the-art spectrophotometric code by Silva et al. (1998). While this approach successfully accounts for a large variety of observables, it falls short by a substantial factor when trying to account for the mm/sub-mm counts. Similarly, Devriendt & Guiderdoni (2000), who used a totally independent semi-analytic model, were forced to introduce an ad hoc galaxy population to reproduce such counts.

The main problem stems from the fact that, although only a handful of redshifts of SCUBA/MAMBO sources have been reliably measured so far, there is growing circumstantial evidence that many (perhaps most) of them are ultraluminous star-forming galaxies at $z \gtrsim 2$ (Bertoldi et al. 2000; Smail et al. 2001; Dunlop 2001a,b; Carilli et al. 2001; Fox et al. 2002; Scott et al. 2002; Webb et al. 2002b). Furthermore, the inferred star formation rates are very high (typically from a few hundreds to $\sim 1000\,\mathrm{M}_{\odot}\,\mathrm{yr}^{-1}$), consistent with those required to build the stellar populations of massive ellipticals on a time-scale $\lesssim 1$ Gyr.

A detailed, astrophysically grounded, model that fully accounts both for the SCUBA/MAMBO counts and for the main aspects of the chemical evolution of spheroidal galaxies (stellar metallicity, luminosity–metallicity relationship, $\alpha$ enhancement), in the framework of the hierarchical clustering scenario, has been presented recently by Granato et al. (2001).

During the active star formation phase, large spheroidal galaxies show up as luminous sub-mm sources, accounting for the SCUBA and MAMBO counts. The subsequent evolution is essentially passive, giving rise to observables resembling those expected according to the 'monolithic' scenario.

As mentioned by Granato et al. (2001), two distinctive features are predicted for SCUBA/MAMBO galaxies. The first one is that those galaxies are highly biased tracers of the matter distribution, and that well-defined links are established between these galaxies and other galaxy populations such as Lyman break galaxies (LBGs) and extremely red objects (EROs), and with active galactic nuclei (AGNs). The second feature is the extremely steep, essentially exponential, decline of the bright tail of (sub)-mm counts.

Studies of clustering properties are particularly challenging in this scenario; if different objects are drawn from the same population of sources, they have to exhibit the same large-scale (and therefore clustering) behaviour. In this context, it is interesting to note that Almaini et al. (2002) have found that SCUBA galaxies and *Chandra* sources (which are mostly AGNs), although showing a small direct overlap, have essentially the same projected distribution on the sky, suggesting an evolutionary connection between the two populations. Hints that LBGs may indeed be the lower-luminosity/lower-mass counterparts to SCUBA sources, as argued by Granato et al. (2001), come from the findings that the most intrinsically luminous LBGs, presenting the highest star formation rate, contain more dust (Pettini et al. 2001) and have stronger clustering (Giavalisco & Dickinson 2001), and that there is a strong cross-correlation among the two populations (Webb et al. 2002a). A first discussion of these issues was offered by Magliocchetti et al. (2001a, hereafter MA2001). In this paper we extend the analysis in two main aspects: (i) the clustering predictions are compared with observational data at 850 and 170 μm; and (ii) the clustering contribution to fluctuations in the background radiation is computed and compared with that of the cosmological signal as well as of the Galactic dust emission.

While clustering deals with the statistics of spatial distribution of spheroids, another most relevant aspect is the predicted distribution in fluxes of these sources, since they are predicted to have an extremely steep decline of the bright tail of mm/sub-mm counts. This is due to the fact that, according to the adopted model, the bulk of star formation in such objects is essentially complete at $z \simeq 2$. The bright counts therefore essentially reflect the high-luminosity tail of the luminosity function. Hints of such a steep decline can possibly be discerned in the recent MAMBO (Bertoldi et al. 2000; Carilli et al. 2001) and SCUBA bright surveys (Borys et al. 2002; Scott et al. 2002).

In the present work we extensively discuss the implications of this aspect on the amount of sources that undergo amplifications due to strong gravitational lensing, focusing on the effect on number counts for fluxes $10\,\mathrm{mJy} \lesssim S_{850\,\mu\mathrm{m}} \lesssim 100\,\mathrm{mJy}$. We show in particular how the fraction of strongly lensed objects with respect to all the contributing populations are generally much more copious than in other (phenomenological) models that also successfully account for SCUBA/MAMBO counts (Rowan-Robinson 2001; Takeuchi et al. 2001; Pearson et al. 2001). We conclude that the measure of the fraction of strongly lensed objects on (sub)-mm counts at the mentioned fluxes is a powerful test for confirming or rejecting the present scenario.

The layout of this paper is as follows. In Section 2 we compare the predictions of the model by Granato et al. (2001) with recent measurements of clustering properties of SCUBA galaxies (Peacock et al. 2000; Scott et al. 2002; Webb et al. 2002b) and draw some conclusions on the cell-to-cell fluctuations of the projected density of sources, found to be strong enough to account for the discrepancies in the number counts observed in different regions of the sky by different groups. In Section 3 we present the power spectra of total intensity fluctuations due to clustering of forming spheroidal galaxies in different channels of the High Frequency Instrument (HFI) on ESA's *Planck* satellite; we compare such spectra with those expected by cosmic microwave background and Galactic dust emission (Finkbeiner, Davis & Schlegel 1999), and derive predictions for the power spectrum of extragalactic background fluctuations at 170 μm, to be compared with the signal detected by Lagache & Puget (2000). Section 4 gives the essential details of our calculations on the effect of lensing on source counts, while in Section 5 we report our predictions for counts of lensed galaxies at mm/sub-mm wavelengths, with reference to those covered by the *Planck*/HFI instrument. Conclusions are presented in Section 6.

Throughout the paper we will assume a cold dark matter flat cosmology with $\Omega_{\Lambda} = 0.7$, $\Omega_{\mathrm{b}}\,h^2 = 0.025$, $H_0 = 100\,h_0$ km s$^{-1}$ Mpc$^{-1}$ with $h_0 = 0.7$ and a *COBE*-normalized $\sigma_8 = 1$. We note, however, that our conclusions are only weakly dependent on the underlying cosmological model.

## 2 CLUSTERING OF HIGH-$z$ FORMING SPHEROIDAL GALAXIES: MODEL PREDICTIONS VERSUS OBSERVATIONS

A crucial test for a galaxy formation model is its ability to describe correctly the large-scale properties of the populations under investigation. In MA2001 we have presented predictions for the clustering of SCUBA sources and their contribution to the total background fluctuations in the sub-mm band, based on the model by Granato et al. (2001). The model has been proven to provide a good fit to the clustering properties of LBGs (Giavalisco et al. 1998), corresponding in our framework to the early evolutionary phases of low- to intermediate-mass spheroidal galaxies.

In this section we extend the analysis of MA2001 and compare the results to the best up-to-date clustering measurements at 850 μm.

We start off with the theoretical expression for the angular two-point correlation function $w(\theta)$:

$$w(\theta) = 2\frac{\int\int_0^\infty N^2(z) b_{\rm eff}^2(M_{\rm min}, z)({\rm d}z/{\rm d}x)\xi(r, z)\,{\rm d}z\,{\rm d}u}{\left[\int_0^\infty N(z)\,{\rm d}z\right]^2} \quad (1)$$

(Peebles 1980), where $\xi(r, z)$ is the spatial mass–mass correlation function (obtained as in Peacock & Dodds 1996; see also Moscardini et al. 1998; Magliocchetti et al. 2000), $x$ is the comoving radial coordinate, $r = (u^2 + x^2\theta^2)^{1/2}$ (for a flat universe and in the small-angle approximation), and $N(z)$ is the number of objects within the shell $(z, z + {\rm d}z)$. The relevant properties of SCUBA galaxies are included in the redshift distribution of sources $N(z)$, and in the bias factor $b_{\rm eff}(M_{\rm min}, z)$.

Trends for the predicted redshift distribution of sources respectively brighter than 1, 10 and 50 mJy are shown in Granato et al. (2001) and MA2001. Independent of the flux limit adopted, all the curves feature a maximum at $z \simeq 3$, while the redshift range spanned progressively becomes narrower as one goes from fainter to brighter objects. We note that our predictions for a very limited number of sources ($\lesssim$10 per cent to 30 per cent) to appear at redshifts $z \lesssim 2$ is in full agreement with all the available data (see e.g. Eales et al. 2000; Smail et al. 2000, 2002; Dunlop 2001a; Webb et al. 2002b).

The effective bias factor $b_{\rm eff}(M_{\rm min}, z)$ of all the dark matter haloes with masses greater than some threshold $M_{\rm min}$ is then obtained by integrating the quantity $b(M, z)$ (whose expression has been taken from Jing 1998) – representing the bias of individual haloes of mass $M$ – weighted by the mass function $n_{\rm SCUBA}(M, z)$ of SCUBA sources:

$$b_{\rm eff}(M_{\rm min}, z) = \frac{\int_{M_{\rm min}}^\infty {\rm d}M\, b(M, z) n_{\rm SCUBA}(M, z)}{\int_{M_{\rm min}}^\infty {\rm d}M\, n_{\rm SCUBA}(M, z)}, \quad (2)$$

with $n_{\rm SCUBA}(M, z) = n(M, z)T_{\rm B}\,/t_{\rm h}$, where $n(M, z)\,{\rm d}M$ is the mass function of haloes (Press & Schechter 1974; Sheth & Tormen 1999), $T_{\rm B}$ is the duration of the star formation burst and $t_{\rm h}$ is the lifetime of the haloes in which these objects reside. Following Lacey & Cole (1993), this last quantity is defined as $t_{\rm h}(M, z) = t_{\rm s}(M, z) - t_{\rm u}(z)$, where $t_{\rm s}(M, z)$ is the survival time of a halo having a mass $M$ at redshift $z$ (i.e. the cosmic time by which the mass of such a halo has doubled due to either accretion or merging), and $t_{\rm u}(z)$ is the age of the Universe at an epoch corresponding to $z$.

The bias factor $b_{\rm eff}$ in equation (2) and the angular correlation function of equation (1) have then been evaluated for three mass ranges: (i) masses in the range $M_{\rm sph} \simeq 10^9$–$10^{10}\,{\rm M}_\odot$, duration of the star formation burst $T_{\rm B} \sim 2$ Gyr, and typical 850-μm fluxes $S \lesssim 1$ mJy; (ii) masses in the range $M_{\rm sph} \simeq 10^{10}$–$10^{11}\,{\rm M}_\odot$ and $T_{\rm B} \sim 1$ Gyr; and (iii) masses in the range $M_{\rm sph} \gtrsim 10^{11}{\rm M}_\odot$, $T_{\rm B} \sim$ 0.5 Gyr, dominating the counts at 850-μm fluxes $S \gtrsim$ 5–10 mJy (note that by $M_{\rm sph}$ we denote the mass in stars at the present time).

Furthermore, we considered two extreme values for the ratio between mass in stars and mass of the host dark halo – $M_{\rm halo}/M_{\rm sph}$ = 100 and 10 – which encompass the range covered by recent estimates for massive objects (McKay et al. 2001; Marinoni & Hudson 2002). Granato et al. (2001) found that this ratio is about 20–30 for the massive objects.

According to our model, sources are expected to be strongly clustered, with a clustering signal that increases for brighter sources and higher values of $M_{\rm halo}/M_{\rm sph}$. From the above discussion it follows that measurements of $w(\theta)$ are in principle able to discriminate among different models for SCUBA galaxies and in particular to determine both their star formation rate, via the amount of baryonic mass actively partaking of the process of star formation, and the duration of the star formation burst.

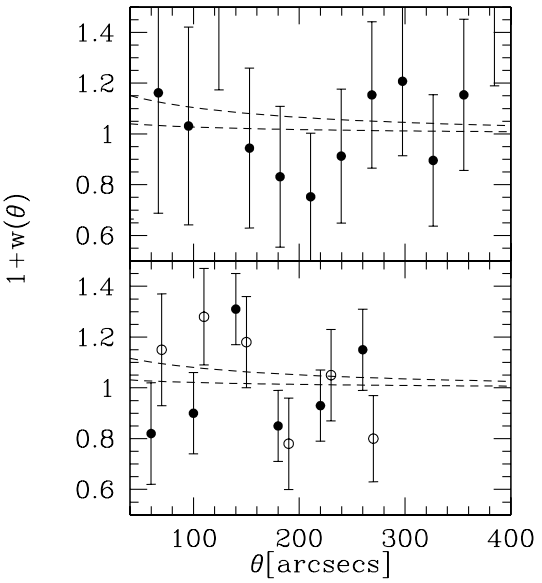


**Figure 1.** Top panel: Angular correlation function of $S \geqslant 5$ mJy SCUBA sources. Model predictions are shown by the dashed curves (where the higher one is for $M_{\rm halo}/M_{\rm sph} = 100$ and the lower one for $M_{\rm halo}/M_{\rm sph} = 10$), while data points represent the Scott et al. (2002) measurements. Bottom panel: Same as above but for sources brighter than 3 mJy. Data are taken from Webb et al. (2002b); empty and filled circles represent measurements obtained in two different fields of the Canada–UK Deep Submillimeter Survey (CUDSS).

In Fig. 1 the angular correlation functions predicted by our model are compared with the recent tentative evidence for positive clustering of SCUBA galaxies with $S_{850\,\mu{\rm m}} \geqslant 5$ mJy (Scott et al. 2002) and with $S_{850\,\mu{\rm m}} \geqslant 3$ mJy (Webb et al. 2002b). Although such measurements are dominated by noise due to the small-number statistics, they suggest the possibility that a future larger sample may provide sharper tests for the models.

Peacock et al. (2000) analysed the contribution of clustering of unresolved ($S < 2$ mJy) SCUBA sources to the 850-μm background fluctuations detected in the *Hubble Deep Field* North (HDF-N). They found some evidence for clustering of the background source population, consistent with an angular correlation function of the form $w(\theta) = (\theta/\theta_0)^{-\epsilon}$, for an a priori value of $\epsilon = 0.8$ and $\theta_0 = 1$ arcsec. Fig. 2 presents our model predictions for the angular correlation function $w(\theta)$ derived in the case of SCUBA galaxies with $S < 2$ mJy; the redshift distribution spans the range $0.7 \lesssim z \lesssim 6$.

Our results are fully consistent with the constraints on structure in the submillimetre background set by Peacock et al. (2000) and not far from their preferred clustering model (dotted line in Fig. 2), if $M_{\rm halo}/M_{\rm sph} = 100$. The shallower slope predicted by our model at small angles ($\theta \lesssim 4 \times 10^{-2}$ deg) ultimately stems from the fact that at high $z$ we enter the regime of linear growth of density perturbations. This entails a flattening of the slope of the two-point spatial correlation function $\xi(r, z)$ for $z \gtrsim 2$. As a consequence, the angular correlation function $w(\theta)$ obtained as in equation (1) by projecting $\xi(r, z)$ over a wide range of redshifts, up to $z \simeq 6$, will mirror this tendency to flatten out. On the other hand, we cannot exclude the presence of a non-linear and/or scale-dependent bias (see e.g. Dekel & Lahav 1999; Blanton et al. 1999; Narayanan, Berlind &

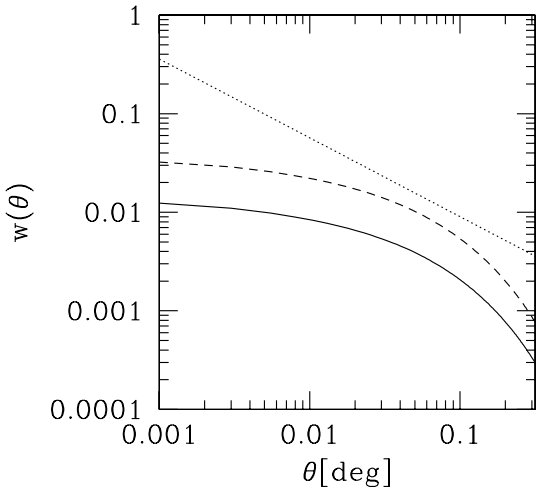


**Figure 2.** Angular clustering of unresolved ($S < 2$ mJy) sources at 850 μm. The solid curve is obtained for $M_{\rm halo}/M_{\rm sph} = 10$, while the dashed one represents the case $M_{\rm halo}/M_{\rm sph} = 100$. The dotted line corresponds to $w(\theta) = (\theta/1\ {\rm arcsec})^{-0.8}$ (Peacock et al. 2000).

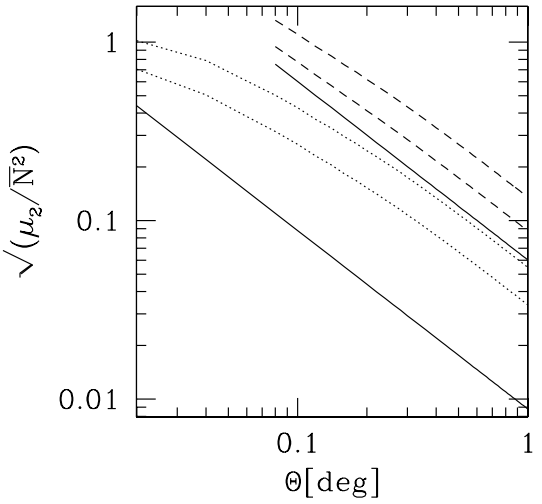


**Figure 3.** Predictions for the rms fluctuations relative to the Poisson noise of detected sources per cell of area $\omega = \Theta^2$, $\mu_2^{1/2}/\bar{N}$, at 850μm. Dashed and dotted curves are for sources brighter than 10 or 1 mJy, respectively. Higher curves of each type correspond to $M_{\rm halo}/M_{\rm sph} = 100$, lower ones to $M_{\rm halo}/M_{\rm sph} = 10$. The solid lines show the Poisson contributions for the two flux limits. The lines are drawn only for angular scales such that the mean number of sources in the solid angle $\omega = \Theta^2$ is $\geqslant 1$.

Weinberg 2000) at the small physical scales probed by the Peacock et al. (2000) sample, which could raise the slope of the angular correlation function up to values closer to the standard −0.8.

Strong clustering substantially enhances cell-to-cell fluctuations of the surface density of detected sources. The angular correlation function $w(\theta)$ is in fact related to the second moment (variance) of the galaxy distribution function via the expression (Peebles 1980; Roche & Eales 1999)

$$\mu_2 = \bar{N} + \left(\frac{\bar{N}}{\omega}\right)^2 \Sigma^2, \tag{3}$$

where $\mu_2$ is the total variance of the source distribution, $\bar{N}$ (the mean count of sources in the solid angle $\omega$) represents the Poisson noise arising from the discrete nature of the objects, and the normalized variance $\Sigma^2$ can be written as

$$\Sigma^2 = \int w(\theta)\, {\rm d}\omega_1\, {\rm d}\omega_2. \tag{4}$$

In the case of square cells with $\omega = \Theta \times \Theta$, equation (4) can be expressed as the two-dimensional integral

$$\Sigma^2(\Theta) = \Theta^2 \int_0^\Theta {\rm d}x \int_0^\Theta w(\theta)\, {\rm d}y, \tag{5}$$

with $\theta = \sqrt{x^2 + y^2}$.

The quantity in equation (5) has been evaluated for the three cases of low-, intermediate- and high-mass SCUBA galaxies, introduced in this section and based on the Granato et al. (2001) model, and for the usual two different values of the $M_{\rm halo}/M_{\rm sph}$ ratio. Results for the rms fluctuations relative to the mean number of detected sources per cell, $\mu_2^{1/2}/\bar{N}$ (see equation 3) are presented in Fig. 3, where dashed and dotted curves respectively correspond to sources brighter than 10 and 1 mJy. We have adopted a mean surface density per square degree of $\bar{N} = 180$ for a flux limit of 10 mJy (see Scott et al. 2002), and of $\bar{N} = 1.3 \times 10^4$ for a flux limit of 1 mJy (Granato et al. 2001). Fig. 3 clearly illustrates that the contributions to cell-to-cell fluctuations due to clustering are generally at least comparable to, and may be much larger than, the Poisson ones, shown by the two solid lines. We therefore conclude that the high clustering amplitude predicted for SCUBA sources can easily account for the differences found in the number counts observed in different sky regions by different groups (see e.g. Smail, Ivison & Blain 1997; Hughes et al. 1998; Blain et al. 1999; Barger, Cowie & Sanders 1999a; Eales et al. 2000; Scott et al. 2002). On the other hand, currently available samples are too small to allow an unambiguous recognition of the effect of clustering. From equation (3) we estimate that an observational determination of the cell-to-cell variance due to clustering, as predicted by the model, would require a survey of a few times $10^{-2}$ deg$^2$ if the source detection limit is 1 mJy and of $\simeq$1 deg$^2$ for a detection limit of 10 mJy.

## 3 MULTIWAVELENGTH ANALYSIS OF THE CONTRIBUTION OF CLUSTERING TO BACKGROUND FLUCTUATIONS

The strong clustering of high-$z$ forming spheroidal galaxies adds an important contribution to background fluctuations. Measurements of such a contribution can be informative on both the nature and the properties of sources below the detection limit. On the other hand, these fluctuations may have a significant impact on the detectability of cosmic microwave background (CMB) fluctuations.

MA2001 (but see also Scott & White 1999; Haiman & Knox 2000) estimated the power spectrum of clustering fluctuations at 850 μm. In the present section we apply the same analysis to different wavelengths, corresponding to the effective frequencies of the channels of the *Planck*/HFI instrument: 2100 μm → 143 GHz; 1380 μm → 217 GHz; 550 μm → 545 GHz; 350 μm → 857 GHz. We also work out predictions at λ = 170 μm, the wavelength probed by the FIRBACK deep survey (Dole et al. 2001).

The counts of spheroidal galaxies are obtained from the model by Granato et al. (2001). The counts of spiral and starburst galaxies at all the wavelengths relevant to this work have been instead estimated by extrapolating the 60-μm local luminosity functions of these two populations (Saunders et al. 1990), and evolving them in luminosity as $L(z) = L(0)\ (1 + z)^\alpha$, with $\alpha = 3.5$ in the case of starbursts and $\alpha = 0$ for spirals. The extrapolation in frequency has been carried out

adopting the observed spectral energy distributions of NGC 6946 and 6090, respectively, in the case of spirals and starburst galaxies (see Silva et al. 1998). No evolution is assumed for spiral galaxies in keeping with the notion of almost constant star formation rate in discs, at least in the last 6–7 Gyr, corresponding to $z \leqslant 0.5$. The evolution of the starburst population, i.e. $\alpha = 3.5$, is instead fixed by the fits to the 175 and 60 μm counts. It is worth noticing that the starburst and spiral counts at $S_{850\,\mu\mathrm{m}} \geqslant 5$–10 mJy are almost fixed by the observed 175 μm counts.

The contribution to the counts of forming spheroidal galaxies, compared to that of spiral and starburst galaxies, is found to decrease for decreasing wavelength because of the increasingly less favourable *k*-corrections associated with the former population. Spirals and starbursts consequently become more and more important at shorter and shorter wavelengths, and eventually dominate the counts for $\lambda \lesssim 200\,\mu$m. This is illustrated by Fig. 4, where we show the contribution to the integral number counts (represented by the solid curves) of the three populations of spheroidal galaxies (dot-dashed lines), spirals (dashed lines) and starbursts (dotted lines) at different wavelengths.

Fig. 4 shows that, under our assumptions, starbursts and spirals constitute a negligible fraction of the total number of sources at mm/sub-mm wavelengths, the dominant contribution coming from high-$z$ forming spheroidal galaxies [the same which – according to Granato et al. (2001) – show up as SCUBA sources at $\lambda = 850\,\mu$m] at all but very bright fluxes (with a flux threshold that varies with wavelength), where, as already discussed in the introduction and extensively tackled in Section 4, the number counts of spheroidal galaxies experience an exponential decline. The situation is reversed at 175 μm (bottom right panel of Fig. 4) where, down to fluxes $S_{175\,\mu\mathrm{m}} \simeq 0.3$ mJy, spirals and starbursts dominate the predicted number counts. In the following analysis we will therefore only consider the population of spheroidal galaxies when dealing with the mm/sub-mm wavelength range.

The angular correlation function of intensity fluctuations due to inhomogeneities in the space distribution of unresolved sources (i.e. with fluxes fainter than some threshold $S_\mathrm{d}$), $C(\theta)$, can be expressed as the sum of two terms, $C_\mathrm{p}$ and $C_\mathrm{c}$, the first one due to Poisson noise (fluctuations given by randomly distributed objects), and the second one due to source clustering (see MA2001 and De Zotti et al. 1996, for a detailed discussion). In the case of highly clustered sources such as forming spheroidal galaxies, the Poisson term $C_\mathrm{p}$ is found (see e.g. Scott & White 1999) to be negligible when compared to $C_\mathrm{c}$. We can therefore safely assume $C \simeq C_\mathrm{c}$, whose expression is given by

$$C_\mathrm{c}(\theta) = \left(\frac{1}{4\pi}\right)^2 \int_{z(L_\mathrm{min},\,S_\mathrm{d})}^{z_\mathrm{max}} \mathrm{d}z\, b_\mathrm{eff}^2(M_\mathrm{min}, z) \frac{j_\mathrm{eff}^2(z)}{(1+z)^4} \left(\frac{\mathrm{d}x}{\mathrm{d}z}\right)^2 \times \int_0^\infty \mathrm{d}(\delta z)\, \xi(r, z), \tag{6}$$

where $b_\mathrm{eff}(M_\mathrm{min}, z)$ is defined by equation (2), $x$ is the comoving radial coordinate, $\delta z = c/H_0 u$ [$u$ is introduced in equation (1) and $c$ is the speed of light], $z_\mathrm{max}$ is the redshift when the sources begin to shine, $z(L, S_\mathrm{d})$ is the redshift at which a source of luminosity $L$ is seen with a flux equal to the detection limit $S_\mathrm{d}$, and $j_\mathrm{eff}$ is the effective volume emissivity.

Following the MA2001 approach, $C_\mathrm{c}(\theta)$ in equation (6) has then been evaluated separately for the three cases of low-, intermediate- and high-mass objects, and the total contribution of clustering to intensity fluctuations $C^\mathrm{tot}(\theta)$ has been derived by adding up in quadrature all the values of $C_\mathrm{c}(\theta)$ obtained for the different mass intervals and by also taking into account the cross-correlation terms between objects of different masses.

The angular power spectrum of the intensity fluctuations can then be obtained as

$$C_l = \left\langle \left| a_l^0 \right|^2 \right\rangle = \int_0^{2\pi} \int_0^\pi [\delta T(\theta)]^2\, P_l(\cos\theta) \sin\theta\, \mathrm{d}\theta\, \mathrm{d}\phi, \tag{7}$$

with

$$\delta T(\theta) = \langle (\Delta T)^2 \rangle^{1/2} = \frac{\lambda^2 \sqrt{C^\mathrm{tot}(\theta)}}{2k_\mathrm{b}} \left[\exp\left(\frac{h\nu}{k_\mathrm{b}T}\right) - 1\right]^2 \times \exp\left(-\frac{h\nu}{k_\mathrm{b}T}\right) \Big/ \left(\frac{h\nu}{k_\mathrm{b}T}\right)^2, \tag{8}$$

which relates intensity and brightness total intensity fluctuations.

This analysis has been performed for the different central frequencies of the *Planck*/HFI, and Fig. 5 shows the results in terms of $\delta T_l = \sqrt{l(l+1)C_l/2\pi}$ (in units of K) at 2100, 1380, 550 and 350 μm. In each of the four panels of Fig. 5, dotted curves are obtained by adopting the $5\sigma$ detection limits of the different *Planck* channels ($S_\mathrm{lim} = 300$ mJy at 2100 μm, $S_\mathrm{lim} = 200$ mJy at 1380 μm, $S_\mathrm{lim} = 450$ mJy at 550 μm, $S_\mathrm{lim} = 700$ mJy at 350 μm) estimated by Toffolatti et al. (1998). In Fig. 6 we also plot predictions for temperature fluctuations at 850 μm, where the contribution from star-forming spheroidals has been corrected for a programming mistake affecting the numerical calculations by MA2001, which produced wiggles in the trend of the predicted power spectrum for multipoles $l \gtrsim 200$. The dotted curves are obtained for a source detection limit of $S_\mathrm{lim} = 100$ mJy, while the dashed ones illustrate the case of a 10 times higher sensitivity ($S_\mathrm{d} = 0.1 S_\mathrm{lim}$). Note that the clustering signal is very weakly dependent on the detection limit for fluxes brighter than ∼5–10 mJy, i.e. for all those sources on the steep portion of the counts (see Fig. 4). Because of this, the results shown in Fig. 6 are also representative in the case of surveys with detection limits higher than 100 mJy, as will probably be the case for the Planck mission. On the other hand, other forthcoming large-area surveys (see e.g. the BLAST project, Devlin et al. 2001)[1] can go substantially deeper than *Planck* over limited areas of the sky.

The solid curves in Figs 5 and 6 show, for comparison, the power spectrum of primary CMB anisotropies corresponding to a flat ΛCDM cosmology, calculated with the CMBFAST code developed by Seljak & Zaldarriaga (1996). The relative importance of fluctuations due to clustering rapidly increases with decreasing wavelength. CMB anisotropies on small angular scales are exceeded at all wavelengths $\lambda \leqslant 850\,\mu$m. This high clustering signal mostly comes from massive galaxies with bright fluxes, which lie at substantial redshifts and are therefore highly biased tracers of the underlying mass distribution. Also the negative *k*-corrections increase their contribution to the effective volume emissivity (see MA2001) and therefore to the fluctuations.

This implies that important information on the clustering properties of faint submillimetre/far-infrared (sub-mm/far-IR) galaxies (and hence on physical properties such as their mass and/or the amount of baryons involved in the star formation process) will reside in the *Planck* maps at frequencies greater than 353 GHz where, however, the dominant diffuse signal at those frequencies is expected to come from interstellar dust emission.

[1] www.hep.upenn.edu/blast/

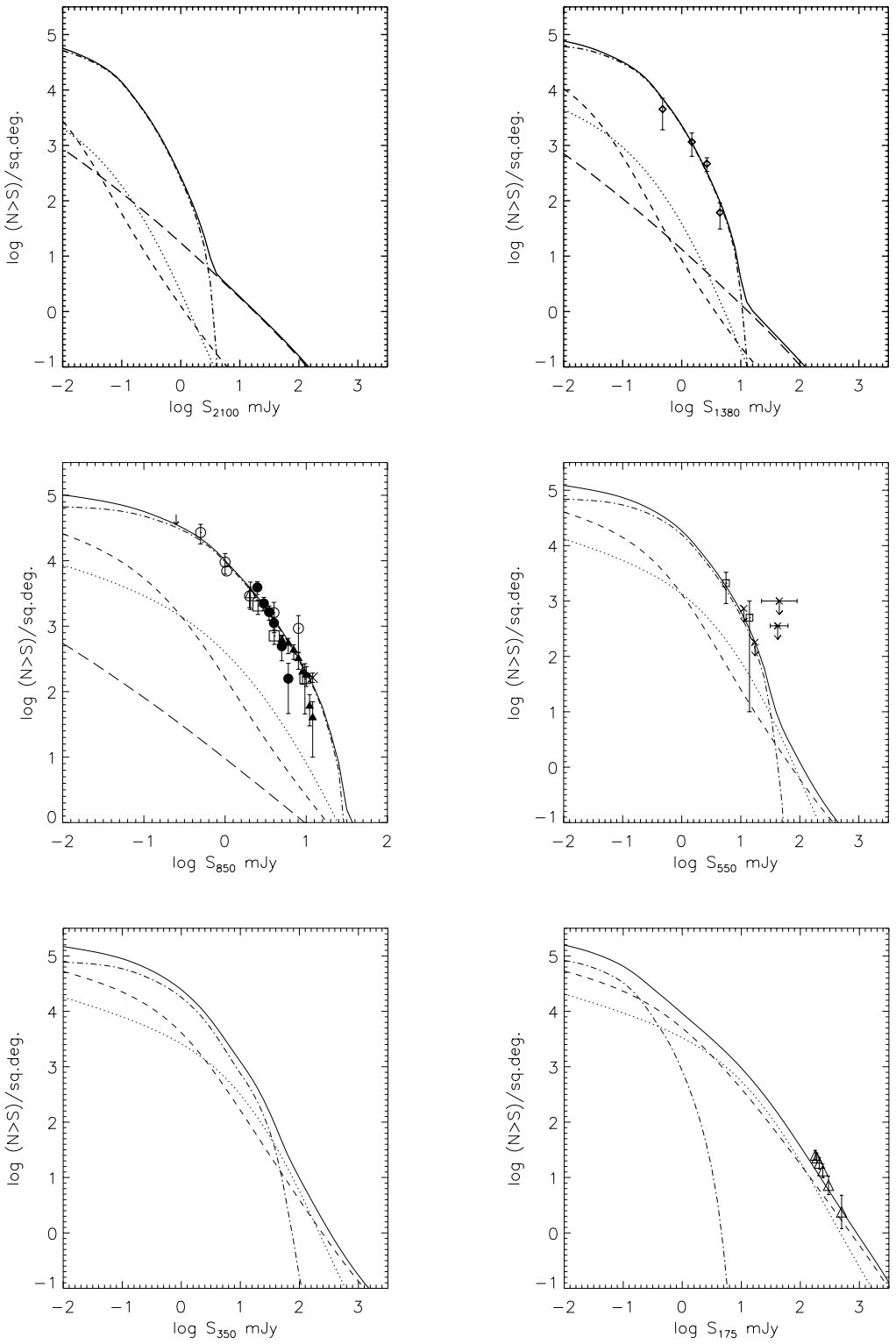


**Figure 4.** Integral number counts of galaxies predicted by the model of Granato et al. (2001) at $\lambda = 2100$ μm (top left-hand panel), 1380 μm (top right-hand panel), 850 μm (middle left-hand panel), 550 μm (middle right-hand panel), 350 μm (bottom left-hand panel) and 175 μm (bottom right-hand panel). The solid curves show the total counts, while the dot-dashed, dashed and dotted curves are respectively obtained for the three populations of forming spheroidals, of spirals and of starburst galaxies. The long-dashed curves (only for $\lambda \geqslant 850$ μm) show the counts of radio sources based on the model by Toffolatti et al. (1998). Data in the 1380 μm panel are derived from MAMBO observations (Bertoldi et al. 2001); a flux density ratio $S_{1200\,\mu m}/S_{1380\,\mu m} = 1.5$ has been adopted to extrapolate to $\lambda = 1.38$ mm the MAMBO flux densities at $\lambda = 1.2$ mm (according to the model, this ratio varies between 1.4 and 1.6, depending on the details of the dust temperature distribution). Data at 175 μm are from Dole et al. (2001). Data at 850 μm are from Blain et al. (1999) (open circles), Hughes et al. (1998) (open triangles), Barger et al. (1999a) (open squares), Eales et al. (2000) (filled circles), Scott et al. (2002) (filled triangles) and Borys et al. (2001) (crosses). Data at 550 μm are an extrapolation of the 450 μm observations by Smail et al. (1997), Barger et al. (1998), Hughes et al. (1998), Eales et al. (1999) and Blain et al. (2000); a mean ratio $S_{450\,\mu m}/S_{550\,\mu m} = 1.78$, typical for spiral and starburst galaxies, has been adopted.

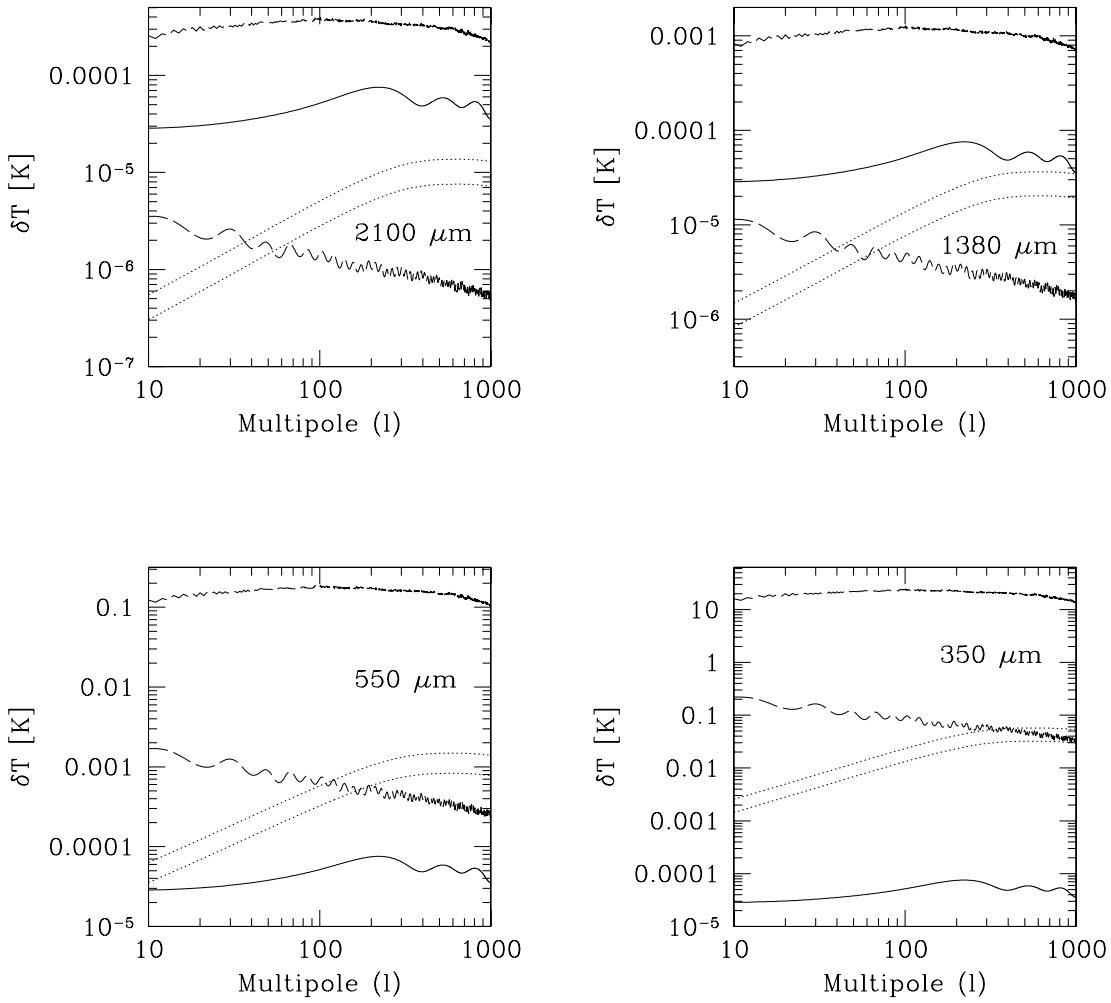


**Figure 5.** Predicted power spectrum of temperature fluctuations $\delta T_l$ (in units of K) as a function of the multipole $l$ at 2100 μm (top-left panel), 1380 μm (top-right panel), 550 μm (bottom-left panel) and 350 μm (bottom-right panel), the central frequencies of the *Planck*/HFI channels. The dotted curves are for the $5\sigma$ flux detection limit of each channel. Higher curves of the same kind are for $M_{\rm halo}/M_{\rm sph} = 100$, lower ones for $M_{\rm halo}/M_{\rm sph} = 10$. The solid curves represent the power spectrum of primary CMB anisotropies as predicted by a standard ΛCDM cosmology ($\Omega_\Lambda = 0.7$, $\Omega_0 = 0.3$, $h_0 = 0.7$). The upper long-dashed curves represent the contribution from Galactic dust emission averaged over all the sky, while the lower ones correspond to high Galactic latitudes ($|b| \geqslant 80^\circ$) only. The clustering signal is potentially detectable at several wavelengths by a high-sensitivity experiment like *Planck*/HFI in regions of low Galactic dust emission, particularly after application of efficient component separation algorithms. Its contamination of CMB maps is, however, small at 2100 μm, and at 1380 μm may be important only on small scales. On the other hand, foregrounds dominate over the CMB for $\lambda \leqslant 550$ μm.

In order to quantify this last effect, we have calculated the expected contribution of Galactic dust emission to background fluctuations. To this end, the full-sky dust emission maps at submillimetre and microwave wavelengths constructed by Finkbeiner et al. (1999) from *IRAS* and *COBE* (DIRBE and FIRAS) data have been used.

Fig. 5 shows the power spectrum of Galactic dust emission averaged all over the sky (upper long-dashed curves). This signal dominates at all wavelengths because of the large contribution from the Galactic plane. However, it is still possible to detect the clustering signal of sub-mm galaxies (and also recover the CMB power spectrum for $\lambda \gtrsim 10^3$ μm) if one restricts the analysis to low-dust regions, e.g. to high enough Galactic latitude regions (i.e. $|b| \geqslant 80^\circ$, lower long-dashed curves).

It turns out that, for both $\lambda = 850$ μm (see also Magliocchetti et al. 2001b) and $\lambda = 550$ μm, the dust contribution in these regions becomes less important than the one due to the clustering of unresolved sources at any $l \gtrsim 100$. For $\lambda = 350$ μm the signal due to Galactic dust is instead found to hide all the other sources of background fluctuations at all Galactic latitudes, except possibly in the case of very high ($l \gtrsim 800$) multipoles.

Background fluctuations due to unresolved extragalactic sources have recently been measured by Lagache & Puget (2000) at 170 μm in a field covered by the FIRBACK survey with ISOPHOT (Dole et al. 2001). As already mentioned, in this case the dominant contribution to counts and to small-scale fluctuations is expected, according to our model, to come from low- to intermediate-redshift spiral and starburst galaxies, whose bias factor $b_{\rm eff}(M_{\rm min}, z)$ appearing in equation (6) takes the form

$$b(z) = 1 + \frac{b_0 - 1}{D(z)} \tag{9}$$

(Fry 1996; see also Baugh et al. 1999; Magliocchetti et al. 1999, 2000), independent of the mass of the haloes hosting such sources and merely a function of redshift – via the linear growth rate $D(z)$ – and of the local bias $b_0 \equiv b(z = 0) = \sigma_{8,\rm g}/\sigma_8$, where $\sigma_{8,\rm g}$ is the rms

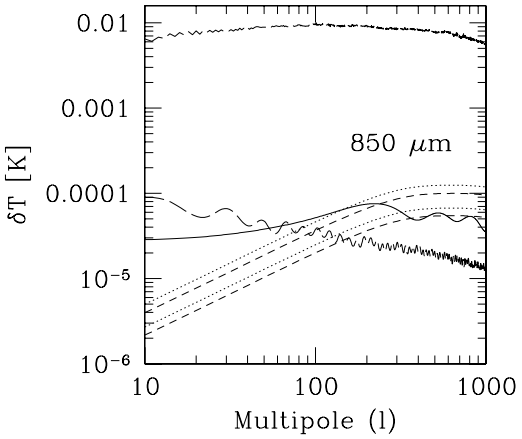


**Figure 6.** As in Fig. 5, but for the 850 μm case. Dotted curves are for a detection limit $S_d = 100$ mJy, while dashed ones are for $S_d = 10$ mJy. Higher curves of the same kind are for $M_{halo}/M_{sph} = 100$, lower ones for $M_{halo}/M_{sph} = 10$.

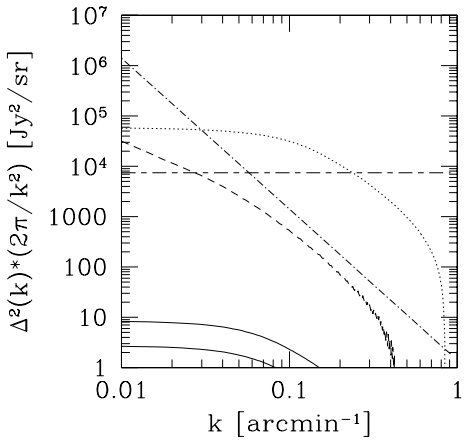


**Figure 7.** Predictions for the power spectrum of intensity fluctuations due to clustering of galaxies fainter than a detection limit $S_d = 135$ mJy at $\lambda = 170$ μm. The solid curves are for the population of spheroidal galaxies (the higher one referring to $M_{halo}/M_{sph} = 100$, the lower one to $M_{halo}/M_{sph} = 10$), while the dashed and dotted curves respectively show the predictions for spiral and starburst galaxies. The short/long-dashed curve represents a white noise power spectrum $P_p = 7400$ Jy$^2$ sr$^{-1}$, while the dashed-dotted one illustrates the cirrus confusion noise (both from Lagache & Puget 2000).

fluctuation amplitude in a sphere of radius 8 $h^{-1}$ Mpc as measured in the local Universe for each population. We have estimated the amplitudes $\sigma_{8,g}$ from the clustering properties by spectral type determined by Loveday, Tresse & Maddox (1999) from Stromlo-APM survey data. We find $\sigma_{8,g} = 0.93$ for galaxies with weak emission lines (spirals) and $\sigma_{8,g} = 0.66$ for galaxies with strong emission lines (starbursts).

The contribution of clustering to $C(\theta)$ has then been calculated for the three populations of spheroidals, spirals and starbursts, and the angular power spectrum $\Delta^2(k)$ has been derived according to the expression (see Peacock 1997)

$$\Delta^2(k) = k^2 \int_0^\infty C(\theta) J_0(k\theta)\theta \, \mathrm{d}\theta, \qquad (10)$$

where $k$ is the angular wavenumber and $J_0$ is the zeroth-order Bessel function. The results for a detection limit $S_d = 135$ mJy, corresponding to three times the confusion noise of the FIRBACK survey (Dole et al. 2001), are shown in Fig. 7. As expected, the contribution of spheroidal galaxies at this wavelength is negligible when compared to those originating from the clustering of both starburst galaxies and spirals. Also, despite the strongly negative bias, the signal obtained for starbursts turns out to be stronger than the one predicted for spiral galaxies, as a result of the different evolutionary properties of the two populations, as outlined above.

The horizontal short/long-dashed line in Fig. 7 represents the Poisson contribution $P_p = 7400$ Jy$^2$ sr$^{-1}$ derived from the Guiderdoni et al. (1997) predictions, while the dashed-dotted line illustrates the contribution to the observed power spectrum of the Galactic cirrus (Lagache & Puget 2000). According to our predictions, fluctuations stemming from the clustering of starburst galaxies are detectable above other sources of signal in the wavenumber range $0.04 \lesssim k\,(\mathrm{arcmin}^{-1}) \lesssim 0.3$.

## 4 GRAVITATIONAL LENSING

It is now well established (Franceschini et al. 1991, 1994, 2001; Blain & Longair 1993; Pearson & Rowan-Robinson 1996; Guiderdoni et al. 1997, 1998; Dwek et al. 1998; Blain et al. 1999; Devriendt & Guiderdoni 2000; Pearson et al. 2001; Takeuchi et al. 2001; Rowan-Robinson 2001) that the coupling of the strongly negative $k$-correction at mm/sub-mm wavelengths – due to the steep increase with frequency of dust emission in galaxies – with the strong cosmological evolution demonstrated both by the *ISO* and SCUBA data (Smail et al. 1997; Hughes et al. 1998; Elbaz et al. 1999; Barger et al. 1999a; Eales et al. 2000) and by the intensity of the far-IR background (Puget et al. 1996; Fixsen et al. 1998; Schlegel, Finkbeiner & Davis 1998; Hauser et al. 1998; Lagache et al. 1999, 2000), greatly emphasizes high-redshift sources. This yields very steep counts which maximize the magnification bias and lead to a high probability for such sources to be gravitationally lensed (Peacock 1982; Turner, Ostriker & Gott 1984). As already discussed by Blain (1996, 1997, 1998a,b, 1999, 2000), this corresponds to a fraction of lensed sources expected to show up in the mm/sub-mm band which is much larger than what is found in surveys at other wavelengths. For instance, Blain (1998a) predicts about 0.6 to 5 per cent of the point sources observed in the future by *Planck*/HFI to be lensed.

As first noted in Perrotta et al. (2002), a distinctive feature of the astrophysically grounded model by Granato et al. (2001) is that both the lensing probability and the magnification bias at mm/sub-mm wavelengths are substantially higher than those implied by other current, mostly phenomenological, models which also successfully account for SCUBA/MAMBO counts (Rowan-Robinson 2001; Takeuchi et al. 2001; Pearson et al. 2001). This is because, according to this model, most galaxies detected in blank-field SCUBA and MAMBO surveys are interpreted as massive ellipticals at $z \gtrsim 2$, in the process of building their stellar populations with very high star formation rates (typically from a few hundreds to $\sim$1000 $\mathrm{M}_\odot\,\mathrm{yr}^{-1}$). Thus, on the one hand, the optical depth to lensing is, on average, significantly higher than for most of the other models, which generally predict a substantial fraction of objects to be at $z < 2$. On the other hand, the model entails an extremely steep, essentially exponential, decline of the bright tail of mm/sub-mm counts of this galaxy population due to the fact that dust emission from these objects rapidly fades away at $z \lesssim 2$ when the bulk of their star formation is essentially over (Cohen 2001). The bright counts therefore somehow reflect the high-luminosity tail of the luminosity function, which

in turn reflects the fact that, in the hierarchical clustering scenario, massive haloes are exponentially rare at high redshifts [note that a similar redshift distribution for the SCUBA sources and similar source counts have been obtained in the parametric model of Blain et al. (1999) with an empirical approach].

Such a steep decrease of the number counts for fluxes 10 mJy $\lesssim S_{850\,\mu\mathrm{m}} \lesssim$ 100 mJy implies a large fraction of strongly lensed galaxies to appear at bright mm/sub-mm fluxes. Indeed, in Perrotta et al. (2002) we have shown that strongly lensed spheroid counts actually come to dominate the unlensed ones at fluxes of about 100 mJy, and at 850 μm wavelength. We provide here a detailed assessment of this promising result, quantifying the fraction of strongly lensed (sub)-mm sources when taking into account all the contributing populations at different wavelengths and giving a quantitative comparison with phenomenological models successfully accounting for SCUBA/MAMBO counts.

Let us first recall the main aspects of our model for gravitational lensing, referring to our previous work (Perrotta et al. 2002) for details. Lensing statistics is expressed by the probability for a source at redshift $z_\mathrm{s}$ to be lensed with magnification $\geqslant\mu$: it is obtained by dividing the total lensing cross-section by the area of the source sphere as

$$P(\mu, z_\mathrm{s}) = \frac{(1+z_\mathrm{s})^2}{4\pi r^2(z_\mathrm{s})} \int_0^{z_\mathrm{s}} \mathrm{d}z \frac{\mathrm{d}V}{\mathrm{d}z}(1+z)^3 \times \int \mathrm{d}M\, \sigma(\mu, z, z_\mathrm{s}, M) \frac{\mathrm{d}n}{\mathrm{d}M}(z, M), \quad (11)$$

where $r(z)$ is the comoving radial distance to redshift $z$, $\mathrm{d}V/\mathrm{d}z$ is the proper volume element per unit redshift, and $\mathrm{d}n(z, M)/\mathrm{d}M$ is the comoving number density of the lenses. Since we are dealing with gravitational lensing by dark matter haloes, we assume that the lens distribution follows the Sheth & Tormen (1999) mass function

$$\frac{\mathrm{d}n}{\mathrm{d}M} = \sqrt{\frac{2aA^2}{\pi}} \frac{\rho_0}{M^2} \frac{\delta_\mathrm{c}(z)}{\sigma(M)} \left\{1 + \left[\frac{\sigma(M)}{\sqrt{a}\,\delta_\mathrm{c}(z)}\right]^{2p}\right\} \times \left|\frac{\mathrm{d}\ln\sigma}{\mathrm{d}\ln M}\right| \exp\left[-\frac{a\delta_\mathrm{c}^2(z)}{2\sigma(M)^2}\right], \quad (12)$$

where the best-fitting values of the parameters for our cosmological model are $a = 0.707$, $p = 0.3$ and $A \simeq 0.3222$. Here $\rho_0$ is the mean mass density at a reference epoch $t_0$, which we assume to be the present time, and $\sigma^2$ is the variance of linear density fluctuations at the present epoch, smoothed with a spherical top-hat filter $W_R(k)$ enclosing a mass $M$. Finally, $\delta_\mathrm{c}^2(z)$ is the linear density contrast of an object virializing at $z$, linearly evolved to the present epoch.

Quite independent of the lens model, $P(\mu, z)$ decreases as $\mu^{-2}$ for $\mu \gg 1$, and hence the high-magnification tail of the probability per unit magnification can be written as $p(\mu, z) = -\mathrm{d}P(\mu, z)/\mathrm{d}\mu \propto a(z)\mu^{-3}$. Equation (11) assumes non-overlapping cross-sections, which is satisfied in the $P \ll 1$ regime, i.e. when no more than a single clump causes lensing of a background source: this results in magnifications markedly larger than unity, or strong lensing. Smaller magnifications, including demagnifications, attain contributions from the distribution of dark matter along the entire line of sight, resulting in weak lensing effects. The latter case can be represented by a Gaussian probability per unit magnification:

$$p(\mu, z) = H(z) \exp\left[-(\mu - \bar{\mu})^2 / 2\sigma_\mu^2(z)\right], \quad (13)$$

where the location of the peak, $\bar{\mu}$, and the amplitude, $H(z)$, are determined by the normalization and flux conservation conditions obtained by integrating over all possible magnifications the combined (weak plus strong lensing) probability distribution: $\int \mathrm{d}\mu\, p(\mu, z) = \int \mathrm{d}\mu\, \mu p(\mu, z) = 1$. The dispersion $\sigma_\mu(z)$ is discussed by Bartelmann & Schneider (2001). The transition between the weak and strong lensing regimes is set at a suitable magnification $\mu_\mathrm{cut}$: a convenient choice is $\mu_\mathrm{cut} = 1 + 1.5\,\sigma_\mu(z)$, yielding $\mu_\mathrm{cut} \approx 1.5$–2 for the redshift range of interest.

In the case of extended sources we must allow for a magnification cut-off, determined by the intrinsic brightness profile of the source (Peacock 1982), by the mass density profile of the lens, and by the geometry of the source/lens system. We follow the approach by Peacock (1982) and introduce a cut-off factor in the magnification distribution of the form $\exp(-\mu/\mu_\mathrm{max})$. As shown by Perrotta et al. (2002), for a typical brightness profile of a luminous elliptical galaxy with $r_\mathrm{e} \simeq 5$ kpc, we expect $10 \leqslant \mu_\mathrm{max} \leqslant 30$, depending on the detailed geometry of the source and the lens and on their relative distance. The still scanty information on sizes of sub-mm galaxies (Downes et al. 1999; Gear et al. 2000; Ivison et al. 2001) suggests radii of a few kiloparsecs, implying higher maximum magnifications. On the other hand, if the SCUBA/MAMBO galaxies are really merging systems of galaxies up to 30 kpc in diameter, then the limiting magnification will be lower. For $r_\mathrm{e} \simeq 15$ kpc, we verified numerically that, using the same assumptions, one gets a maximum amplification between 5 (for elliptical lens potential) and 10 (for circular lens potential). Therefore, we adopted a relatively conservative value $\mu_\mathrm{max} = 10$.

Lens density profiles have been modelled as singular isothermal spheres (SIS) for masses $M < 3.5 \times 10^{13}\,\mathrm{M}_\odot$, and with the Navarro, Frenk & White (1997, hereafter NFW) formula for larger masses. In fact, it is found (Porciani & Madau 2000) that such a 'mixed' model provides a good fit to the observed statistics of the angular splitting of quasar multiple gravitational images. However, we wish to emphasize that, regarding statistical magnifications, SIS and NFW profiles lead to comparable results (Perrotta et al. 2002), making the present conclusions very weakly dependent on the choice of the profile.

Before moving to the results, let us consider the magnification bias on a flux-limited source sample. The integrated source counts above a flux density threshold $S_\nu$ of sources with a comoving luminosity function $\Phi(L, z)$ can be written as (e.g. De Zotti et al. 1996)

$$N(S_\nu) = \int_0^{z_0} \mathrm{d}z \int_{L_\mathrm{min}}^\infty \mathrm{d}L\, \Phi(L, z) r^2(z) \frac{\mathrm{d}r}{\mathrm{d}z}\ \mathrm{sr}^{-1}, \quad (14)$$

where $r$ is the comoving radial distance, and

$$L_\mathrm{min}(\nu) = 4\pi(1+z) r^2(z) S_\nu \frac{L(\nu)}{L((1+z)\nu)}. \quad (15)$$

The luminosity function modified by the magnification bias reads (e.g. Pei 1995)

$$\Phi'(L, z) = \int_{\mu_\mathrm{min}}^\infty \mathrm{d}\mu\, \frac{p(\mu, z)}{\mu} \Phi(L/\mu, z). \quad (16)$$

Lensing effects on the source counts are taken into account by replacing $\Phi'(L, z)$ with $\Phi(L, z)$ in equation (14).

## 5 EFFECT OF GRAVITATIONAL LENSING ON SOURCE COUNTS

We present here our estimates for the effect of lensing on the integral number counts predicted using the model by Granato et al. (2001), at different wavelengths, focusing on the strongly lensed source fraction when all the contributing populations are taken into

account; for comparison with different scenarios, we use the model by Rowan-Robinson (2001), taken as representative of successful phenomenological models. The model by Granato et al. (2001) includes three populations, namely star-forming spheroids, evolving starburst galaxies and non-evolving disc galaxies (spirals). The model by Rowan-Robinson instead includes AGNs, spirals and both high- and low-luminosity starburst galaxies. In both models, we added the contribution due to 'flat'-spectrum radio sources, whose counts (kindly provided by L. Toffolatti) are based on the model by Toffolatti et al. (1998).

The contributions of different populations to the number counts at fluxes probed by SCUBA, predicted by the two models, are markedly different: While, as discussed above, according to Granato et al. (2001), SCUBA sources are mostly massive dusty spheroids at high $z$, in many phenomenological models there is a large tail extending to low $z$, so that the mean lensing probability of sources is lower. Correspondingly, while the model by Granato et al. (2001) predicts an essentially exponential decline of the 850-μm counts with increasing flux density above a few millijansky, the slope is substantially less steep in the Rowan-Robinson (2001) model.

This different behaviour of the counts and of the redshift distributions explains the vastly different fractions of lensed galaxies expected at bright fluxes; this difference is quantified in Figs 8 and 9, as we describe in detail in the following. Both figures show the integral number counts of lensed and unlensed galaxies, yielded by the two models, respectively, for the 550 (top), 850 (middle) and 1380 μm (bottom) *Planck*/HFI channels. Fig. 8 shows the unlensed, weakly lensed and strongly lensed spheroid counts, represented respectively by light dotted, heavy dashed and heavy solid curves. The heavy dotted curve represents the sum over all the populations that are expected to contribute to the observed counts according to the Granato et al. (2001) model, i.e. spheroids, evolving starburst galaxies, spirals and radio sources, assuming no lensing effects. In Fig. 9 the light dotted, heavy dashed and heavy solid curves represent respectively the unlensed, weakly lensed and strongly lensed counts for the sum of AGNs, spirals and starbursts. As above, the heavy dotted curve represents the sum of the contributions from all the populations plus radio sources, assuming no lensing effects. Note that for the model by Granato et al. (2001) we plotted the effect of lensing only on the forming spheroids to highlight the huge magnification bias due to the steepness of the counts, while starburst galaxies, spirals and radio sources, which are negligibly affected by lensing, are included only in the total counts, represented in Fig. 8 by the heavy dotted curves. In the case of Rowan-Robinson (2001), for all classes of sources (AGNs, spirals and starburst galaxies) the effect of lensing has been taken into account. The heavy dotted curves give the sum of weakly and strongly lensed sources, plus the contribution of radio sources, for which the effect of lensing is negligible.

It is clear from Fig. 8 that, according to the model by Granato et al. (2001) and as a result of the strong magnifications due to gravitational lensing, forming spheroids at substantial redshifts can be detected in relatively shallow surveys, such as those provided by *Planck*/HFI. The quoted $5\sigma$ detection limits for this instrument are $S_{\rm lim} = 200$, 100 and 450 mJy at 1380, 850 and 550 μm, respectively. Note that, at 850 μm, this implies that the expected strongly lensed objects at fluxes larger than $S_{\rm lim}$ on the whole sky are $\sim 10^2$ in the Rowan-Robinson (2001) scenario and $\sim 4 \times 10^3$ according to the model by Granato et al. (2001). Strongly lensed forming spheroids may also be detectable by forthcoming balloon experiments operating at sub-mm wavelengths, such as BLAST (Devlin et al. 2001)[2] and ELISA (Ristorcelli et al. 2001). Such surveys may then trace the large-scale distribution of the peaks of the primordial density field. The distribution of strongly lensed sources would extend to even higher fluxes in the case of magnifications larger than our conservative limit $\mu_{\rm max} = 10$ [magnifications of up to 30 are possible according to the adopted model (cf. Perrotta et al. 2002)].

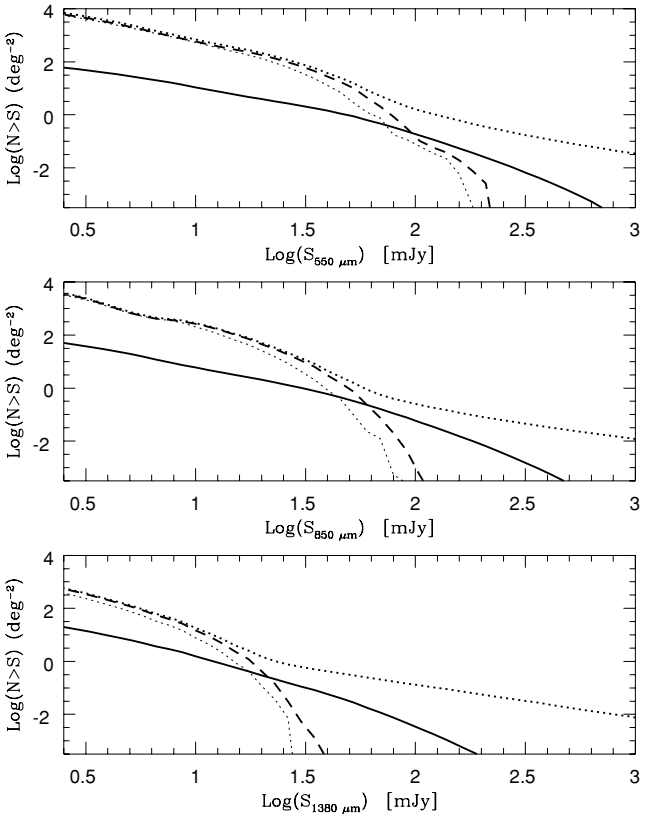


**Figure 8.** Integral source counts per square degree for the model by Granato et al. (2001) at 550 (top), 850 (middle) and 1380 μm (bottom). The dashed and solid curves respectively refer to the weakly lensed (including the case of flux demagnification) and strongly lensed counts of forming spheroids only; the light dotted curve shows, for comparison, the counts of such sources as predicted by the model without taking lensing into account. The heavy dotted curves show the total counts after allowing for the effect of lensing on the counts of forming spheroids and including contributions from populations whose counts are essentially unaffected by lensing (such as 'flat'-spectrum radio sources), as described in the text.

A basic observable to compare the effect of strong lensing in the two scenarios is the ratio

$$\mathcal{R} = N_{\rm strong}/N, \tag{17}$$

where $N_{\rm strong}$ represents the counts due to strongly lensed objects only, while $N$ contains all sources from all populations without taking into account the strong lensing effect. In other words, $\mathcal{R}$ is the ratio between the heavy solid and the heavy dotted curves in Figs 8 and 9. Fig. 10 shows this ratio as a function of the 850-μm flux predicted by the two models considered above. According to the model by Granato et al. (2001), at 850 μm the ratio of strongly lensed to unlensed sources reaches the value of about 40 per cent for fluxes slightly below 100 mJy, where the surface density of strongly lensed sources is of about 0.1 deg$^{-2}$. Note, however, that the actual fraction

[2] www.hep.upenn.edu/blast/

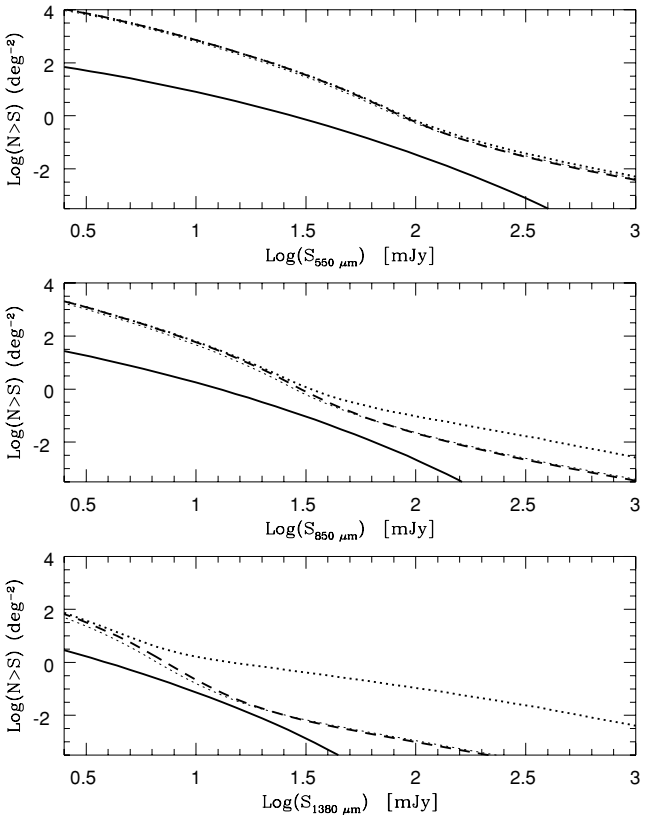


**Figure 9.** Integral source counts for the model by Rowan-Robinson (2001). The meaning of the curves is analogous to that in Fig. 8. In this case, however, the light dotted, the dashed (almost superimposed on the dotted), and the solid curves include the contributions of all the populations considered by Rowan-Robinson. The heavy dotted curve also includes 'flat'-spectrum radio sources for which the effect of lensing is negligible.

of strongly lensed sources may be even higher than shown in Fig. 10. In fact we stress that, in a way which is consistent with the available observational constraints, the scenario in Fig. 8 maximizes the contributions to the counts from spiral and starburst galaxies. Indeed, the counts due to these sources at bright fluxes are significantly higher than those predicted by Rowan-Robinson (2001), as can be seen by comparison with Fig. 9 (radio sources are the same in both models). Thus we emphasize that a large fraction of strongly lensed sources is expected at $S_{850\,\mu\mathrm{m}} \simeq 100$ mJy even under conservative assumptions about the dilution by unlensed populations. On the other hand, the fraction of strongly lensed sources is expected to lie below 10 per cent for the many phenomenological models, as is the case for the model of Rowan-Robinson (2001) (see Fig. 10). As we already stressed, this difference is mainly due to the fact that in this scenario the SCUBA/MAMBO galaxies belong to populations that are present up to very low redshifts, being therefore negligibly affected by gravitational lensing. For comparison with the results on strong lensing effects, we also plot in Fig. 11 the ratio between the total (strongly and weakly) lensed counts, and the unlensed ones (i.e. without taking into account any lensing effect), at 850 μm. For the model by Granato et al. (2001), the classes of sources that contribute to the counts include spheroids, starburst galaxies, spirals and radio sources. However, only the spheroids undergo significant strong lensing, the other sources being only weakly lensed due to their relatively low redshift. For the plot relative to the Rowan-Robinson model, the lensed source counts include AGN, spiral, starburst and

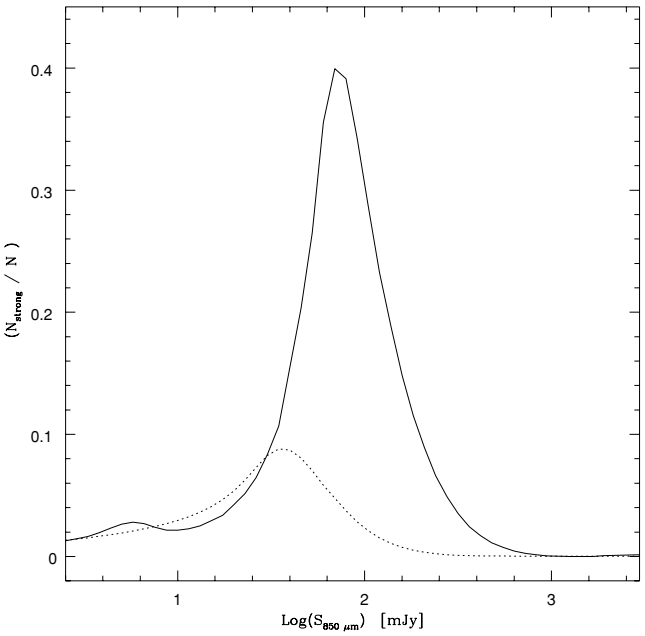


**Figure 10.** Ratio of strongly lensed to unlensed counts at 850 μm: the solid curve refers to the model by Granato et al. (2001), the dotted curve to the one by Rowan-Robinson (2001).

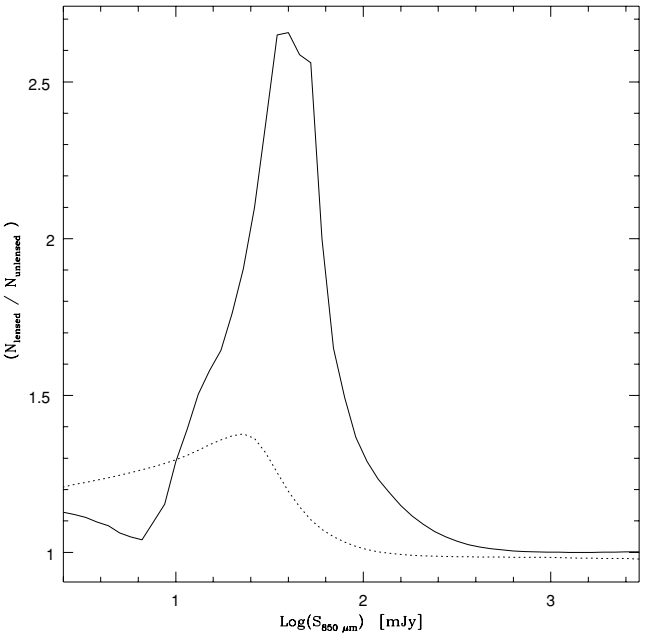


**Figure 11.** Ratio of total (strongly and weakly) lensed to unlensed counts at 850 μm: again, the solid curve refers to the model by Granato et al. (2001), the dotted curve to the one by Rowan-Robinson (2001).

'flat'-spectrum radio sources, for which the dominant contribution is due to weak lensing. We see from Fig. 11 that at low fluxes (say, $<10$ mJy) the fraction of lensed sources detectable in a flux-limited survey is slightly higher in the Rowan-Robinson model than in the Granato model, mainly because of the contribution by weakly lensed sources. On the other hand, this ratio increases at higher fluxes for the Granato et al. (2001) model, because, as we have seen, in this flux region the contribution from strongly lensed spheroids is mostly enhanced.

It is then clear that gravitational lensing can help to discriminate among different models, all of them successfully reproducing the observed counts. Note that the strongly lensed sources detected by shallow submillimetre surveys, such as those carried out by *Planck*/HFI, are characterized, according to our model, by having $z > 2$ (typically, $z \simeq 3$), while most unlensed dusty (spiral and starburst) galaxies are at $z \lesssim 1$. The different populations can therefore be sifted based on the multifrequency *Planck*/HFI data as a result of their different sub-mm colours. A promising method to diagnose whether sub-mm sources are lensed has recently been proposed and discussed by Chapman et al. (2002), who estimated that the fraction of strongly lensed SCUBA sources is 3–5 per cent at ~10 mJy. Although in the flux interval covered by SCUBA surveys it is difficult to discriminate among the models discussed in the present paper, the method could give interesting indications if applied to larger-area surveys, i.e. to brighter fluxes (see Fig. 10).

In principle, clustered lenses can change the clustering properties of the sources in a flux-limited sample. The autocorrelation function of the lensing magnification pattern can be described as a convolution of the magnification pattern of a single lens with the correlation function of the lens centres. In our case, the magnification patterns of individual lenses have typical angular scales of at most a few arcseconds. The autocorrelation of lens centres, however, has a typical angular scale of arcminutes, and its amplitude is substantially lowered by projection because the lens population is taken from a large redshift range. Therefore, the effect of lensing on the clustering properties of sub-mm sources is negligible.

Weak lensing, however, can modify the autocorrelation function of a flux-limited source sample, in particular if the source counts drop as steeply with increasing flux as in the Granato et al. (2001) model. The intrinsic correlation function $w(\theta)$ of the sources then becomes $w(\theta) + (\alpha - 1)^2\, w_\mu(\theta)$, where $w_\mu(\theta)$ is the magnification autocorrelation function due to weak lensing, and $\alpha$ is defined as $-\mathrm{d}\ln\ N(>S)/\mathrm{d}\ln\ S$ in the neighbourhood of the flux limit of the observation. Typical amplitudes of $w_\mu(\theta)$ for high-redshift sources are of the order of 0.1, and the angular scale of $w_\mu(\theta)$ is of the order of a few arcminutes (e.g. Bartelmann & Schneider 2001). At the same time, weak lensing will cause cross-correlations between the background sources and foreground galaxies because the latter are correlated with the weakly lensing dark matter distribution (e.g. Dolag & Bartelmann 1997; Moessner & Jain 1998). Using this additional effect, it will be possible to disentangle the lensing-induced and the intrinsic source autocorrelations.

## 6 CONCLUSIONS

A major challenge for current theories of galaxy formation is to account for the evolutionary history of large spheroidal galaxies. Observations presently suggest that most of the stars (say >60–70 per cent) in large ellipticals were assembled at early epochs $z \simeq 2$ (Eales et al. 1999; Daddi et al. 2000; Cohen 2001; see Peebles 2002 for a review). On the basis of their sub-mm properties and follow-up at other wavelengths, sources detected by SCUBA and MAMBO have been associated with starbursting proto-ellipticals (e.g. Dunlop 2001b; Scott et al. 2002).

Even the most recent semi-analytic models (Cole et al. 2000; Devriendt & Guiderdoni 2000), which hinge upon the 'standard' picture for structure formation in the framework of the hierarchical clustering paradigm, tuned to agree with detailed numerical simulations, are unable to account for the sub-mm counts of galaxies as well as for an early ($z \simeq 2$) formation of most large ellipticals.

On the other hand, Granato et al. (2001) pointed out that the feedback from supernovae yields a star formation rate (SFR) increasing with the final mass in stars $M_{\rm sph}$ as SFR $\simeq 100(M_{\rm sph}/10^{11}\mathrm{M}_\odot)^{1.33}\,\mathrm{M}_\odot\,\mathrm{yr}^{-1}$. As a consequence, according to this model, the formation of stars in small galaxies is delayed with respect to large ellipticals: the latter evolve on very small time-scales (similar to those assumed in 'monolithic' models) and the mm/sub-mm counts are successfully reproduced. The star formation activity, powering the dust emission, quickly declines for $z < 3$ for the most luminous (most massive) galaxies, while quasars reach their maximum luminosity. This naturally explains why very luminous quasars are more easily detected at mm/sub-mm wavelengths at redshifts larger than that ($\simeq$2.5) of maximum quasar activity (Omont et al. 2001). As indicated by the analysis of the latter authors, a substantial fraction of the observed far-IR emission is probably powered by the starburst in the host galaxy.

In this paper statistical properties of clustering and lensing of the proto-ellipticals predicted by the model are extensively investigated and compared with recent data. Attention is focused, in particular, on two specific aspects. Since SCUBA/MAMBO galaxies are interpreted as massive galaxies at $2 \lesssim z \lesssim 6$, they are expected to be highly biased tracers of the matter distribution and therefore highly clustered. The implied angular correlation function is found to be consistent with recent results by Peacock et al. (2000), Lagache & Puget (2000), Scott et al. (2002) and Webb et al. (2002b), as well as with the fluctuations in the SCUBA counts in different areas of the sky. Explicit estimates are presented for the power spectrum of temperature fluctuations due to clustering in *Planck*/HFI channels.

A second specific prediction of the model is an essentially exponential decline of the counts at $S_{850\,\mu\mathrm{m}} \gtrsim 10$ mJy up to the fluxes at which spirals, starbursts and radio sources show up. Hints in this direction that can possibly be discerned in recent SCUBA (Borys et al. 2002; Scott et al. 2002) and MAMBO (Carilli et al. 2001) surveys are noted. As an implication of this prediction, together with the fact that sources are found at high redshifts, one has that both the gravitational lensing probability and the magnification bias on the counts are much higher than those derived for other current, phenomenological, models. We show that, according to this model, essentially all proto-spheroidal galaxies brighter than $S_{850\,\mu\mathrm{m}} \gtrsim 60$–70 mJy are gravitationally lensed. Allowing for the other populations of sources contributing to the bright mm/sub-mm counts, we find that the fraction of gravitationally lensed sources may be $\simeq$40 per cent at fluxes slightly below $S_{850\,\mu\mathrm{m}} = 100$ mJy. If so, large-area surveys such as those to be carried out by *Planck*/HFI or by forthcoming balloon experiments like BLAST and ELISA will probe the large-scale distribution of the peaks of the primordial density field. The multifrequency observations provided by *Planck* will help in discriminating between high-redshift sources (with high lensing probability), relatively nearby starburst and spiral galaxies, and radio sources.

## ACKNOWLEDGMENTS

We are grateful to P. Panuzzo and L. Toffolatti for help with the counts of spheroidal galaxies and radio sources, respectively. This work was supported in part by ASI, MURST and UE.

## REFERENCES

Almaini O. et al., 2002, astro-ph/0108400
Barger A. J., Cowie L. L., Sanders D. B., Fulton E., Taniguchi Y., Sato Y., Kawara K., Okuda H., 1998, Nat, 394, 248
Barger A. J., Cowie L. L., Sanders D. B., 1999a, ApJ, 518, L5

Barger A. J., Cowie L. L., Trentham N., Fulton E., Hu E. M., Songaila A., Hall D., 1999b, AJ, 117, 102
Bartelmann M., Schneider P., 2001, Phys. Rep., 340, 291
Baugh C. M., Cole S., Frenk C. S., Lacey C. G., 1998, ApJ, 498, 504
Baugh C. M., Benson A. J., Cole S., Frenk C. S., Lacey C. G., 1999, MNRAS, 305, 21
Benitez N., Broadhurst T. J., Bouwens R. J., Silk J., Rosati P., 1999, ApJ, 515, L65
Bertoldi F. et al., 2000, A&A, 360, 92
Bertoldi F., Menten K. M., Kreysa E., Carilli C. L., Owen F., 2001, in Wilner D. J., ed., Highlights of Astronomy Vol. 12. Astron. Soc. Pac., San Francisco
Blain A. W., 1996, MNRAS, 283, 1340
Blain A. W., 1997, MNRAS, 290, 553
Blain A. W., 1998a, MNRAS, 295, 92
Blain A. W., 1998b, MNRAS, 297, 511
Blain A. W., 1999, MNRAS, 304, 669
Blain A. W., 2000, in Kneib J.-P., Mellier Y., Moniez M., Tran Thanh Van J., eds, Rencontres de Moriond XX, Cosmological Physics with Gravitational Lensing. Editions Frontières, Gif sur Yvette (astro-ph/0007196)
Blain A. W., Longair M. S., 1993, MNRAS, 264, 509
Blain A. W., Smail I., Ivison R. J., Kneib J.-P., 1999, MNRAS, 302, 632
Blain A. W., Ivison R. J., Kneib J.-P., Smail I., 2000, in Bunker A. J., van Breughel W. J. M., eds, ASP Conf. Ser. Vol. 193, The Hy-Redshift Universe: Galaxy Formation and Evolution at High Redshift. Astron. Soc. Pac., San Francisco, p. 246
Blanton M., Cen R., Ostriker J. P., Strauss M. A., 1999, ApJ, 522, 590
Borys C., Chapman S., Halpern M., Scott D., 2002, MNRAS, 330, L63
Broadhurst T. J., Bowens R. J., 2000, ApJ, 530, 53
Carilli C. L., Bertoldi F., Bertarini A., Menten K. M., Kreysa E., Zylka R., Owen F., Yun M., 2001, in Lowenthal J., Hughes D. K., eds, Deep Millimeter Surveys: Implications for Galaxy Formation. World Scientific, Singapore
Chapman S. C., Smail I., Ivison R. J., Blain A. W., 2002, MNRAS, 335, L17
Cohen J. G., 2001, AJ, 121, 2895
Cole S., Lacey C. G., Baugh C. M., Carlton M., Frenk C. S., 2000, MNRAS, 319, 168
Daddi E., Cimatti A., Renzini A., 2000, A&A, 362, L45
Dekel A., Lahav O., 1999, ApJ, 520, 24
Devlin M. J., 2001, in Lowenthal J. D., Hughes D. H., eds, Proc. UMass/INAOE Conf. World Scientific, Singapore
Devriendt J. E. G., Guiderdoni B., 2000, A&A, 363, 851
De Zotti G., Franceschini A., Toffolatti L., Mazzei P., Danese L., 1996, Astrophys. Lett. Commun., 35, 289
Dolag K., Bartelmann M., 1997, MNRAS, 291, 446
Dole H. et al., 2001, A&A, 372, 364
Downes D. et al., 1999, A&A, 347, 809
Dunlop J. S., 2001a, New Astron. Rev., 45, 609
Dunlop J. S., 2001b, in Lowenthal J., Hughes D. K., eds, Deep Millimeter Surveys: Implications for Galaxy Formation. World Scientific, Singapore
Dwek E. et al., 1998, ApJ, 508, 106
Eales S., Lilly S., Gear W., Dunne L., Bond J. R., Hammer F., Le Fèvre O., Crampton D., 1999, ApJ, 515, 518
Eales S., Lilly S., Webb T., Dunne L., Gear W., Clements D. L., Yun M., 2000, AJ, 120, 2244
Elbaz D. et al., 1999, A&A, 351, L37
Finkbeiner D. P., Davis M., Schlegel D. J., 1999, ApJ, 524, 867
Fixsen D. J., Dwek E., Mather J. C., Bennett C. L., Shafer R. A., 1998, ApJ, 508, 123
Fox M. J. et al., 2002, MNRAS, 331, 89
Franceschini A., De Zotti G., Toffolatti L., Mazzei P., Danese L., 1991, A&AS, 89, 285
Franceschini A., Mazzei P., De Zotti G., Danese L., 1994, ApJ, 427, 140
Franceschini A., Silva L., Fasano G., Granato G. L., Bressan A., Arnouts S., Danese L., 1998, ApJ, 506, 600
Franceschini A., Aussel H., Cesarsky C. J., Elbaz D., Fadda D., 2001, A&A, 378, 1
Fry J. N., 1996, ApJ, 461, L65
Gear W. K., Lilly S. J., Stevens J. A., Clements D. L., Webb T. M., Eales S. A., Dunne L., 2000, MNRAS, 316, L51
Giavalisco M., Dickinson M., 2001, ApJ, 550, 177
Giavalisco M., Steidel C. C., Adelberger K. L., Dickinson M. E., Pettini M., Kellogg M., 1998, ApJ, 503, 543
Granato G. L., Lacey C. G., Silva L., Bressan A., Baugh C. M., Cole S., Frenk C. S., 2000, ApJ, 542, 710
Granato G. L., Silva L., Monaco P., Panuzzo P., Salucci P., De Zotti G., Danese L., 2001, MNRAS, 324, 757
Guiderdoni B., Bouchet F. R., Puget J. L., Lagache G., Hivon E., 1997, Nat, 390, 257
Guiderdoni B., Hivon E., Bouchet F. R., Maffei B., 1998, MNRAS, 295, 877
Haiman Z., Knox L., 2000, ApJ, 530, 124
Hauser M. G. et al., 1998, ApJ, 508, 25
Hughes D. H. et al., 1998, Nat, 394, 241
Ivison R. J., Smail I., Frayer D. T., Kneib J.-P., Blain A. W., 2001, ApJ, 561, L45
Jing Y. P., 1998, ApJ, 503, L9
Kauffmann G., 1996, MNRAS, 281, 487
Kauffmann G., Charlot S., White S. D. M., 1996, MNRAS, 283, 117
Lacey C., Cole S., 1993, MNRAS, 262, 649
Lagache G., Puget J. L., 2000, A&A, 355, 17
Lagache G., Abergel A., Boulanger F., Désert F. X., Puget J.-L., 1999, A&A, 344, 322
Lagache G., Haffner L. M., Reynolds R. J., Tufte S. L., 2000, A&A, 354, 247
Loveday J., Tresse L., Maddox S. J., 1999, MNRAS, 310, 281
McKay T. A. et al., 2001, ApJ, submitted (astro-ph/0108013)
Magliocchetti M., Maddox S. J., Lahav O., Wall J. V., 1999, MNRAS, 309, 943
Magliocchetti M., Bagla J., Maddox S. J., Lahav O., 2000, MNRAS, 314, 546
Magliocchetti M., Moscardini L., Panuzzo P., Granato G. L., De Zotti G., Danese L., 2001a, MNRAS, 325, 1553 (MA2001)
Magliocchetti M., Moscardini L., De Zotti G., Granato G. L., Danese L., 2001b, in Treyer M., Tresse L., eds, Where's the Matter? Tracing Dark and Bright Matter with the New Generation of Large Scale Surveys, Proc. Conf. 2001 June. Frontier Group, Marseille
Marinoni C., Hudson M. J., 2002, ApJ, 569, 91
Menanteau F., Ellis R. S., Abraham R. G., Barger A. J., Cowie L. L., 1999, MNRAS, 309, 208
Moessner R., Jain B., 1998, MNRAS, 294, L18
Moscardini L., Coles P., Lucchin F., Matarrese S., 1998, MNRAS, 299, 95
Narayanan V. K., Berlind A. A., Weinberg D. H., 2000, ApJ, 528, 1
Navarro J. F., Frenk C. S., White S. D. M., 1997, ApJ, 490, 493 (NFW)
Omont A., Cox P., Bertoldi F., McMahon R. G., Carilli C., Isaak K. G., 2001, A&A, 374, 371
Peacock J. A., 1982, MNRAS, 199, 987
Peacock J. A., 1997, Cosmological Physics. Cambridge Univ. Press, Cambridge
Peacock J. A., Dodds S. J., 1996, MNRAS, 267, 1020
Peacock J. A. et al., 2000, MNRAS, 318, 535
Pearson C. P., Rowan-Robinson M., 1996, MNRAS, 283, 174
Pearson C. P., Matsuhara H., Onaka T., Watarai H., Matsumoto T., 2001, MNRAS, 324, 999
Peebles P. J. E., 1980, The Large-Scale Structure of the Universe. Princeton Univ. Press, Princeton, NJ
Peebles P. J. E., 2002, in Metcalfe N., Shanks T., eds, ASP Conf. Ser. Vol. 283, A New Era in Cosmology. Astron. Soc. Pac., San Francisco, in press (astro-ph/0201015)
Pei Y. C., 1995, ApJ, 440, 485
Perrotta F., Baccigalupi C., Bartelmann M., De Zotti G., Granato G. L., 2002, MNRAS, 329, 445
Pettini M., Shapley A. E., Steidel C. C., Cuby J., Dickinson M., Moorwood A. F. M., Adelberger K. L., Giavalisco M., 2001, ApJ, 554, 981
Porciani C., Madau P., 2000, ApJ, 532, 679
Press W. H., Schechter P., 1974, ApJ, 187, 425

Puget J.-L., Abergel A., Bernard J.-P., Boulanger F., Burton W. B., Desert F.-X., Hartmann D., 1996, A&A, 308, L5
Ristorcelli I. et al., 2001, in Pilbratt G. L., Cernicharo J., Heras A. M., Prusti T., Harris R., eds, The Promise of the Herschel Space Observatory. ESA-SP 460. ESA Publications Division, Noordwijk, p. 301
Roche N., Eales S. A., 1999, MNRAS, 307, 703
Rodighiero G., Franceschini A., Fasano G., 2001, MNRAS, 324, 491
Rowan-Robinson M., 2001, ApJ, 549, 745
Saunders W., Rowan-Robinson M., Lawrence A., Efstathiou G., Kaiser N., Ellis R. S., Frenk C. S., 1990, MNRAS, 242, 318
Schlegel D. J., Finkbeiner D. P., Davis M., 1998, ApJ, 500, 525
Scodeggio M., Silva D., 2000, A&A, 359, 953
Scott D., White M., 1999, A&A, 346, 1
Scott S. E. et al., 2002, MNRAS, 331, 817
Seljak U., Zaldarriaga M., 1996, ApJ, 469, 437
Sheth R. K., Tormen G., 1999, MNRAS, 308, 119
Silva L., Granato G. L., Bressan A., Danese L., 1998, ApJ, 509, 103
Smail I., Ivison R. J., Blain A. W., 1997, ApJ, 490, L5
Smail I., Ivison R. J., Owen F. N., Blain A. W., Kneib J.-P., 2000, ApJ, 528, 612
Smail I., Ivison R. J., Blain A. W., Kneib J.-P., 2001, in Lowenthal J., Hughes D. K., eds, Deep Millimeter Surveys: Implications for Galaxy Formation. World Scientific, Singapore
Smail I., Ivison R. J., Blain A. W., Kneib J.-P., 2002, MNRAS, 331, 495
Takeuchi T. T., Kawabe R., Kohno K., Nakanishi K., Ishii T. T., Hirashita H., Yoshikawa K., 2001, PASP, 113, 586
Toffolatti L., Argueso Gomez F., De Zotti G., Mazzei P., Franceschini A., Danese L., Burigana C., 1998, MNRAS, 297, 117
Totani T., Yoshii J., 1997, ApJ, 501, L177
Treu T., Stiavelli M., 1999, ApJ, 524, L27
Turner E. L., Ostriker J. P., Gott J. R., 1984, ApJ, 284, 1
Webb T. M. et al., 2002a, ApJ, in press
Webb T. M. et al., 2002b, ApJ, submitted (astro-ph/0201180)
Zepf S. E., 1997, Nat, 390, 377

This paper has been typeset from a TEX/LATEX file prepared by the author.